Rapid Communications

Z^0+jet correlation with next-to-leading-order-matched parton-shower and jet-medium interaction in high-energy nuclear collisions

Shan-Liang Zhang,[1] Tan Luo,[1] Xin-Nian Wang,[1,2] and Ben-Wei Zhang[1,*]

[1]*Key Laboratory of Quark and Lepton Physics (MOE) and Institute of Particle Physics, Central China Normal University, Wuhan 430079, China*

[2]*Nuclear Science Division Mailstop 70R0319, Lawrence Berkeley National Laboratory, Berkeley, California 94740, USA*

(Received 17 May 2018; published 1 August 2018)

The impact of jet quenching on Z^0-tagged jets in relativistic heavy-ion collisions at the CERN Large Hadron Collider is investigated. We employ the SHERPA Monte Carlo program that combines next-to-leading-order matrix elements with matched resummation of parton shower to compute the initial Z^0+jet production. The linear Boltzmann transport (LBT) model is then used to simulate the propagation, energy attenuation of, and medium response induced by jet partons in the quark-gluon plasma. With both higher-order corrections and matched soft and collinear radiation as well as a sophisticated treatment of parton energy loss and medium response in LBT, our numerical calculations can provide the best description so far of all available observables of Z^0+jet simultaneously in both proton + proton and Pb+Pb collisions, in particular, the shift of the distribution in transverse momentum asymmetry $x_{jZ} = p_T^{\rm jet}/p_T^Z$, the modification of azimuthal angle correlation in $\Delta\phi_{jZ} = |\phi_{\rm jet} - \phi_Z|$, and the overall suppression of average number of Z^0-tagged jets per boson R_{jZ} at $\sqrt{s} = 5.02$ TeV as measured by the Compact Muon Solenoid experiment. We also show that higher-order corrections to Z^0+jet production play an indispensable role in understanding Z^0+jet azimuthal angle correlation at small and intermediate $\Delta\phi_{jZ}$, and momentum imbalance at small x_{jZ}. Jet quenching of the subleading jets is shown to lead to suppression of the Z^0+jet correlation at small azimuthal angle difference $\Delta\phi_{jZ}$ and at small x_{jZ}.

DOI: 10.1103/PhysRevC.98.021901

Introduction. Jet quenching or suppression of energetic partons due to energy loss in medium has long been proposed to probe properties of the quark-gluon plasma (QGP) in heavy-ion collisions (HICs) [1–22]. Gauge-boson-tagged jet production is regarded as a "golden channel" to study jet quenching [23,24]. The boson will not participate in the strong interactions directly and can be considered as the proxy of the initial energy of the parton before it propagates through the QGP medium and loses energy [25–27]. Though jet production associated with a direct photon in HICs has already been accessible at the BNL Relativistic Heavy-ion Collider (RHIC), the unprecedented energies available at the CERN Large Hadron Collider (LHC) open a new window for Z^0-tagged jet production in HICs, where the Z^0 gauge boson not only escapes the QGP medium unattenuated, but is also free from fragmentation processes due to its very large mass.

Recently the Compact Muon Solenoid (CMS) Collaboration reported the first measurement of Z^0-tagged jet production in both proton + proton (p+p) and Pb+Pb collisions at $\sqrt{s} = 5.02$ TeV at the LHC [28]. Though the CMS data on the Z^0+jet in Pb+Pb collisions can be qualitatively described by several theoretical models, such as GLV [29–31], hybrid model [32], and JEWEL [33], it is still a challenge to quantitatively describe all the available experimental observables of the Z^0+jet simultaneously and their p+p baseline by simulations based on a leading-order (LO) matrix-element (ME) matched parton-shower (PS) event generator. The Z^0+jet azimuthal angle correlation $\Delta\phi_{jZ} = |\phi_{\rm jet} - \phi_Z|$ and the distributions in average number of Z^0-tagged jets $R_{jZ} = N_{jZ}/N_Z$ are in particular very sensitive to QCD higher-order corrections [28,34]. It is therefore of a great advantage to use the next-to-leading order (NLO) pQCD computations of hard scattering complemented with resummation of soft and collinear parton shower and the state-of-the-art simulations of parton propagation in a QGP medium in the study of Z^0+jet correlation in high-energy HICs.

In this Rapid Communication, we report the first numerical study with such a theoretical model: the Monte Carlo program SHERPA [35], which combines the NLO pQCD with resummation of a matched PS, is used for the initial Z^0-tagged jet production, and provides an excellent description of Z^0+jet production in elementary p+p collisions; the parton propagation in QGP medium is simulated by the linear Boltzmann transport (LBT) model [26,36,37] with bulk medium evolution provided by the Berkeley-Wuhan CLVisc 3+1D hydrodynamics [38,39]. We refer to this model as the NLO+PS LBT model. We will confront our results with available data for all four observables of Z^0+jet in both p+p and Pb+Pb collisions: azimuthal correlation $\Delta\phi_{jZ}$, p_T asymmetry x_{jZ} distribution, and its mean value $\langle x_{jZ}\rangle$, as well as the average number of associated jets per Z^0 boson R_{jZ}. We will focus in particular on effects of multiple jets associated with Z^0 and their suppression on the azimuthal correlation and p_T asymmetry in Pb+Pb collisions.

*bwzhang@mail.ccnu.edu.cn

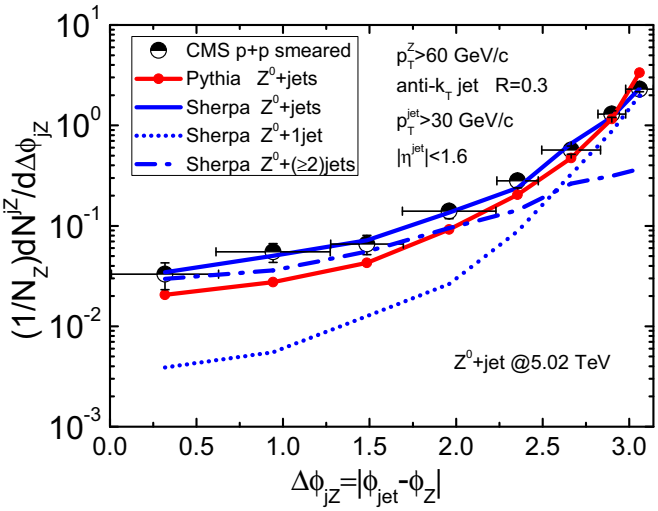

FIG. 1. Comparison between the azimuthal angle correlation $\Delta\phi_{jZ}$ of Z^0+jet by CMS data [28] and theoretical simulations of SHERPA (Blue) and Pythia (Red) in p+p collisions at $\sqrt{s} = 5.02$ TeV. The dotted (the dash-dotted) line shows the contribution from $Z^0 +$ 1jet ($Z^0 + (\geqslant 2)$jets).

SHERPA . SHERPA is a complete Monte Carlo event generator that simulates all high-energy reactions between particles in the standard model. SHERPA employs several merging approaches [40–42] which provide NLO ME matched to the resummation of the Collins-Soper-Sterman [43] dipole PS [44,45] to calculate low jet multiplicities and LO-matched parton showers to simulate high jet multiplicities. The matching scheme can be formulated symbolically as

$$\langle O\rangle^{(\mathrm{NLO+PS})} = \int d\Phi_B[B+\widetilde{V}+I^S](\Phi_B)\widetilde{\mathrm{PS}}_B\left(\mu_Q^2, O\right) + \int d\Phi_R[R(\Phi_R) - D^S(\Phi_B * \Phi_1)] \times \widetilde{\mathrm{PS}}_R(t_R, O), \quad (1)$$

where Φ_B is the Born phase-space, Φ_R is real phase-space, and B, $\widetilde{V}$, and R denote Born, virtual, and real ME, respectively. D^S is the subtraction term which has the same soft divergence as the real terms in the subtraction scheme; $I^S = \int d\Phi_1 D^S$ is the integrated subtraction term. The introduction of D^S and I^S makes both matrix-element part finite. $\widetilde{\mathrm{PS}}_B(\mu_Q^2, O)$ and $\widetilde{\mathrm{PS}}_R(t_R, O)$ is the parton-shower branch for Born phase and real corrected phase space respectively, with μ_Q^2 and t_R the shower starting points [46–48]. In our simulations, the OPENLOOPS program [49] calculates loop-level diagram elements while SHERPA calculates tree-level diagram elements [50,51] and makes phase-space integration with the parton density set "CTEQ14nlo".

We show in Fig. 1 the Z^0+jet correlation in azimuthal angle $\Delta\phi_{jZ}$ in p+p collisions simulated by SHERPA as compared to the default PYTHIA 6.4 result and CMS data [28]. The SHERPA p+p baseline result shows an excellent agreement with experimental data, while PYTHIA 6.4 slightly overshoots the azimuthal distribution at large $\Delta\phi_{jZ} \sim \pi$ and significantly underestimates the distribution by a factor of ∼2 at small $\Delta\phi_{jZ}$. Contributions from Z^0+1 jet and $Z^0+(\geqslant 2)$ jets to the azimuthal correlation in p+p collisions from SHERPA are also shown in Fig. 1. Contributions from $Z^0+(\geqslant 2)$ jets from NLO processes are much broader than that of Z^0+1 jet and dominate the distribution at the small $\Delta\phi_{jZ}$ region. Z^0+1 jet processes contribute mostly in large $\Delta\phi_{jZ}$ regions where soft and collinear radiation from PS dominates.

To obtain the above numerical results and in the rest of this paper, we adopt the kinematic cuts by CMS experiment [28] to select Z^0-tagged jets in both p+p and Pb+Pb collisions. For $Z^0 \to e^+e^-$ decay, electrons are required to have $p_T^e > 20$ GeV, $|\eta^e| < 2.5$ and are excluded in the kinematic region $1.44 < |\eta^e| < 2.47$. For $Z^0 \to \mu^+\mu^-$ decay, kinematic cuts for muons are $p_T^\mu > 10$ GeV, $|\eta^\mu| < 2.4$. Z^0 bosons are reconstructed by opposite-charge electron or muon pairs, with reconstructed mass $70 < M_{ll} < 110$ GeV, and transverse momentum $p_T^Z > 40$ GeV. Jets are constructed by FASTJET [52] from final partons with the anti-k_T algorithm [53] and jet cone size $R \equiv \sqrt{(\Delta\phi)^2 + (\Delta y)^2} = 0.3$. We have neglected the effect of hadronization. All the jets tagged by a boson should pass thresholds of $p_T^{\mathrm{jet}} > 30$ GeV, $|\eta^{\mathrm{jet}}| < 1.6$, and are rejected in a cone of $R < 0.4$ from a lepton to reduce jet energy contamination.

LBT model. In this study, propagation of fast partons in hot QGP is simulated within the LBT model [26,36,37] that includes both elastic and inelastic processes of parton scattering for both jet shower and thermal recoil partons in the QGP. The elastic scattering is described by the linear Boltzmann equation [26,36,37]

$$p_1\partial f_a(p_1) = -\int \frac{d^3p_2}{(2\pi)^3 2E_2}\int \frac{d^3p_3}{(2\pi)^3 2E_3}\int \frac{d^3p_4}{(2\pi)^3 2E_4} \times \frac{1}{2}\sum_{b(c,d)}[f_a(p_1)f_b(p_2) - f_c(p_3)f_d(p_4)]|M_{ab\to cd}|^2 \times S_2(s,t,u)(2\pi)^4\delta^4(p_1+p_2-p_3-p_4), \quad (2)$$

where $f_{i=a,b,c,d}$ are parton phase-space distributions, $|M_{ab\to cd}|$ is the corresponding elastic ME, and $S_2(s,t,u)$ stands for a Lorentz-invariant regulation condition [26,36,37]. The inelastic scattering is described by the higher twist formalism for induced gluon radiation [54–57] as

$$\frac{dN_g}{dxdk_\perp^2dt} = \frac{2\alpha_s C_A P(x)\hat{q}}{\pi k_\perp^4}\left(\frac{k_\perp^2}{k_\perp^2 + x^2M^2}\right)^2 \sin^2\left(\frac{t-t_i}{2\tau_f}\right), \quad (3)$$

where x and $k_\perp$ denote the energy fraction and transverse momentum of the radiated gluon, $P(x)$ the splitting function, $\hat{q}$ the jet transport coefficient, and $\tau_f = 2Ex(1-x)/(k_\perp^2 + x^2M^2)$ the formation time. The information on local temperature and fluid velocity of the dynamically evolving bulk medium is provided by the 3+1D CLVisc hydrodynamical model [38,39] with initial conditions from the AMPT model [58] averaged over 200 events for each centrality. Parameters in the CLVisc are chosen to reproduce experimental data on bulk hadron spectra. The only parameter in the LBT model that controls the strength of parton interaction is strong coupling α_s which

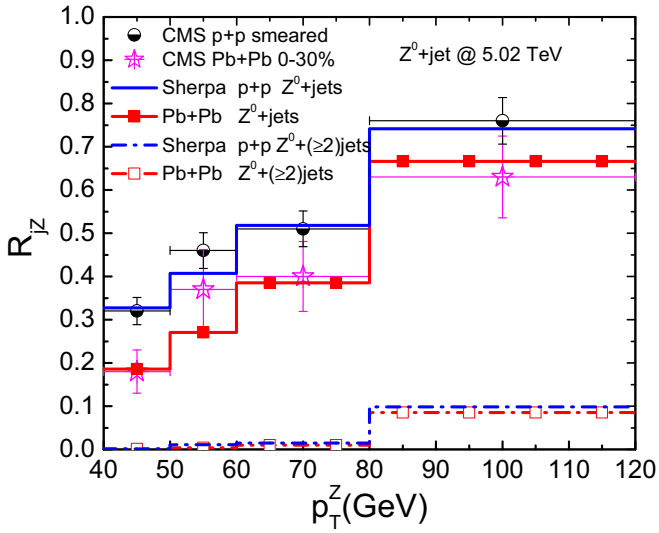

FIG. 2. Calculated R_{jZ} distributions of Z^0+jet as a function of p_T^Z in p+p (blue) and Pb+Pb collisions (red) at $\sqrt{s} = 5.02$ TeV as compared to CMS data [28]. The dash-dotted lines show contributions from $Z^0 + (\geqslant 2)$jets.

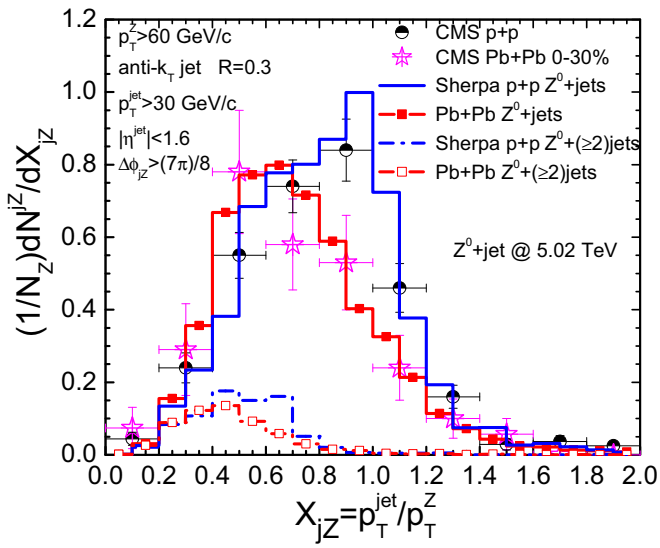

FIG. 3. Calculated momentum imbalance of Z^0+jet in p+p (blue) and Pb+Pb (red) collisions at $\sqrt{s} = 5.02$ TeV as compared to CMS data [28]. The dash-dotted lines show the contributions from $Z^0 + (\geqslant 2)$jets.

is chosen as $\alpha_s = 0.20$ in this study for the best fit of the experimental data. The LBT model has been used to describe successfully several important jet quenching observables, such as photon tagged hadron or jet production, and light and heavy flavor meson suppression [26,36,37,59,60].

Results and discussions. Using the SHERPA NLO+PS event generator and LBT model, we can study medium modification of the Z^0+jet correlation in Pb+Pb at the LHC. Effects of cold nuclear matter are found to be rather small in the kinematics we are interested in [61]. All partons, jet showers, and radiated and medium recoil partons are used for jet reconstruction with FASTJET. In the following calculations of Z^0+jet correlation in Pb+Pb, the underlying events background subtraction has been carried out following the procedure adopted by the CMS experiment [62]. No subtraction is applied in p+p results. The energy and azimuthal angle resolution of the detector are simulated by a Gaussian smearing with centrality-dependent parametrization as given by the CMS experiment [28].

The distribution in average number of tagged jets per Z^0 boson $R_{jZ} = N_{jZ}/N_Z$ is shown in Fig. 2. We note that the jet selection threshold $p_T^{\rm jet} > 30$ GeV imposes a strong constraint on the phase space of Z^0-tagged jets. Significant suppression for R_{jZ} is observed in Pb+Pb collisions relative to that in p+p collisions. This is a direct consequence of jet energy loss that shifts the final transverse momentum of a larger fraction of Z^0-tagged jets below the $p_T^Z = 30$ GeV threshold. The difference between R_{jZ} in p+p and Pb+Pb changes slowly with $p_T^{\rm jet}$. We note that jets with high recoil p_T associated with a Z^0 boson are dominated by quark jets. The contribution of Z^0+ multi-jets to R_{jZ} distribution is small in both p+p and Pb+Pb collisions because of the kinematical constraints of finding multiple high-energy jets whose energy can hardly exceed half of that of the Z^0 boson.

Figure 3 shows our model calculations of the distribution in the transverse momentum asymmetry $x_{jZ} = p_T^{\rm jet}/p_T^Z$ for Z^0-tagged jets at $\sqrt{s} = 5.02$ TeV in p+p and Pb+Pb collisions as compared with CMS data. A cut $\Delta\phi_{jZ} > 7\pi/8$ has been imposed to select the most back-to-back Z^0+jet pairs. Compared to p+p collisions, the asymmetry distribution in x_{jZ} is broadened and shifted toward a smaller value of x_{jZ} in 0–30% central Pb+Pb collisions due to jet energy loss in the QGP medium while the transverse momentum of the Z^0 boson remains the same. The distribution is dominated by the Z^0+1 jet process at large x_{jZ}, but has almost 50% contributions from higher-order corrections at small $x_{jZ} < 0.5$. For completeness we also show our model results on the mean value of momentum imbalance $\langle x_{jZ}\rangle$ at different p_T^Z bins in Fig. 4.

We show in Fig. 5 our calculations of the Z^0+jet correlation in the azimuthal angle difference $\Delta\phi_{jZ}$ between Z^0 bosons and jets in p+p and Pb+Pb collisions at $\sqrt{s} = 5.02$ TeV as compared to CMS data. Note that distributions are normalized by the number of Z^0 events and a kinematic cut $p_T^{\rm jet} > 30$ GeV is imposed for the tagged jets. We observe a moderate suppression of the correlation at small $\Delta\phi_{jZ}$ (large angle relative to the opposite direction of the Z^0 boson) in Pb+Pb relative to that in p+p collisions. This suppression is mainly caused by suppression of subleading jets when energy loss shifts their final transverse momentum below the $p_T^{\rm jet} = 30$ GeV threshold.

To illustrate this mechanism for suppression of small-angle Z^0+jet correlations, we also plot in Fig. 5 contributions from Z^0 plus only one jet (denoted as "$Z^0 + 1$jet") and Z^0 production associated with more than 1 jet (denoted as "$Z^0 + (\geqslant 2)$jets") in p+p and 0–30% central Pb+Pb collisions. We see that for $Z^0 + 1$jet processes, there is no significant difference between the azimuthal distributions in p+p and

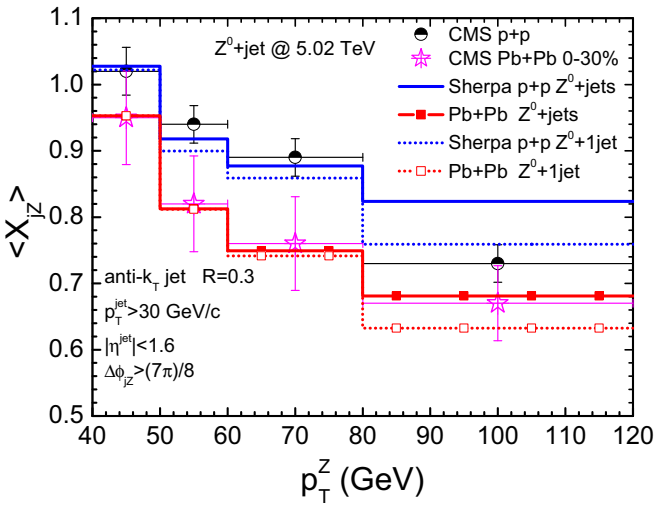

FIG. 4. Numerical calculations on the mean value of x_{jZ} as a function of p_T^Z in p+p (blue) and Pb+Pb (red) collisions at $\sqrt{s} = 5.02$ TeV as compared to the CMS data [28]. The dotted lines show the contributions from $Z^0 + 1$jet.

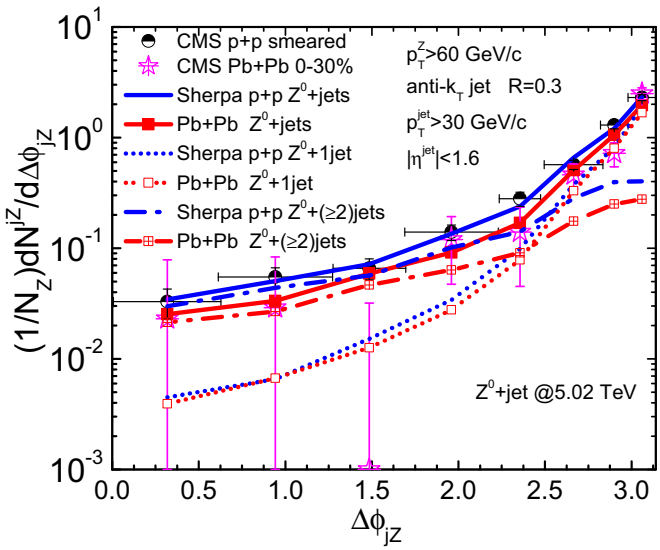

FIG. 5. Numerical results of the azimuthal angle correlation in $\Delta\phi_{jZ}$ in p+p (blue) and Pb+Pb (red) collisions at $\sqrt{s} = 5.02$ TeV as compared to CMS data [28]. The dotted (dash-dotted) lines show the contributions from $Z^0 + 1$jet ($Z^0 + (\geqslant 2)$jets).

Pb+Pb collisions. The Z^0+jet correlation from for $Z^0 + (\geqslant 2)$jets processes, however, is considerably suppressed in Pb+Pb collisions as compared to p+p. In $Z^0 + 1$jet events, the transverse momentum of Z^0 boson is mostly balanced by a back-to-back jet and the Z^0+jet azimuthal correlation is more focused in the $\Delta\phi_{jZ} \sim \pi$ region where the tagged jet has a relatively large energy and is mostly a quark jet. The decorrelation of the Z^0+jet in azimuthal angle from $Z^0 + 1$jet processes in this region is dominated by soft and collinear radiation, the resummation of which can be described by a Sudakov form factor. The transverse momentum broadening of this leading jet due to jet-medium interaction is negligible to that caused by soft and collinear radiation as pointed out in Refs. [18,19,27]. This is why the contribution from $Z^0 + 1$jet events to the azimuthal correlation in Pb+Pb remains almost the same as in p+p. On the other hand, the transverse momentum of Z^0 boson is balanced by multijets in $Z^0 + (\geqslant 2)$jets processes. The initial energy of the tagged jet is much smaller, which can easily fall below $p_T^{\rm jet} = 30$ GeV threshold due to jet energy loss. As we can see in the comparison to the CMS data, future experimental data with much better statistics are needed to observe this suppression of the small-angle Z^0+jet correlation unambiguously.

Summary. We have carried out a systematic study of the Z^0+jet correlation in Pb+Pb collisions at the LHC by combining NLO matrix-element calculations with matched parton shower in SHERPA for initial Z^0+jet production and linear Boltzmann transport model for jet propagation in the expanding QGP from 3+1D hydrodynamics. Results from our model calculations achieve the best agreement so far with the experimental data on all four observables of Z^0+jet production in both p+p and Pb-Pb collisions at LHC: azimuthal correlation in $\Delta\phi_{jZ}$, distribution of transverse momentum imbalance x_{jZ}, the p_T^Z dependence of the mean value $\langle x_{jZ}\rangle$, and the average number of tagged jets per Z^0 boson R_{jZ}. We demonstrate the importance of both higher-order corrections and resummed soft and collinear radiation for a satisfactory description of the available experimental data on Z^0+jet correlations in p+p and Pb+Pb collisions. Energy loss of both leading and subleading jets have to be included consistently to understand the medium modifications of Z^0+jet correlations, in particular in azimuthal angle $\Delta\phi_{jZ}$ and momentum imbalance x_{jZ}.

Acknowledgments. We thank E. Wang, H. Zhang, P. Ru, W. Dai, and S. Chen for helpful discussions. We thank W. Chen for providing 3+1D hydro profile of the bulk medium in our LBT calculation. This work has been supported by NSFC of China with Projects No. 11435004 and No. 11521064, MOST of China under 2014CB845404, NSF under Grant No. ACI-1550228 and U.S. DOE under Contract No. DE-AC02-05CH11231.

[1] X. N. Wang and M. Gyulassy, Phys. Rev. Lett. **68**, 1480 (1992).
[2] M. Gyulassy, I. Vitev, X.-N. Wang, and B.-W. Zhang, *Quark Gluon Plasma 3*, edited by R. C. Hwa *et al.* (World Scientific, Singapore, 2004), pp. 123–191.
[3] G. Y. Qin and X. N. Wang, Int. J. Mod. Phys. E **24**, 1530014 (2015).
[4] I. Vitev, S. Wicks, and B. W. Zhang, J. High Energy Phys. 11 (2008) 093.
[5] I. Vitev and B. W. Zhang, Phys. Rev. Lett. **104**, 132001 (2010).
[6] G. Y. Qin and B. Muller, Phys. Rev. Lett. **106**, 162302 (2011).
[7] J. Casalderrey-Solana, J. G. Milhano, and U. A. Wiedemann, J. Phys. G **38**, 035006 (2011).

[8] C. Young, B. Schenke, S. Jeon, and C. Gale, Phys. Rev. C **84**, 024907 (2011).
[9] Y. He, I. Vitev, and B. W. Zhang, Phys. Lett. B **713**, 224 (2012).
[10] C. E. Coleman-Smith and B. Muller, Phys. Rev. C **86**, 054901 (2012).
[11] K. C. Zapp, F. Krauss, and U. A. Wiedemann, J. High Energy Phys. 03 (2013) 080.
[12] G. L. Ma, Phys. Rev. C **87**, 064901 (2013).
[13] F. Senzel, O. Fochler, J. Uphoff, Z. Xu, and C. Greiner, J. Phys. G **42**, 115104 (2015).
[14] J. Casalderrey-Solana, D. C. Gulhan, J. G. Milhano, D. Pablos, and K. Rajagopal, J. High Energy Phys. 10 (2014) 019; 09 (2015) 175.
[15] J. G. Milhano and K. C. Zapp, Eur. Phys. J. C **76**, 288 (2016).
[16] N. B. Chang and G. Y. Qin, Phys. Rev. C **94**, 024902 (2016).
[17] A. Majumder and J. Putschke, Phys. Rev. C **93**, 054909 (2016).
[18] L. Chen, G.-Y. Qin, S.-Y. Wei, B.-W. Xiao, and H.-Z. Zhang, Phys. Lett. B **782**, 773 (2018).
[19] L. Chen, G. Y. Qin, S. Y. Wei, B. W. Xiao, and H. Z. Zhang, Phys. Lett. B **773**, 672 (2017).
[20] Y. T. Chien and I. Vitev, Phys. Rev. Lett. **119**, 112301 (2017).
[21] L. Apolinário, J. G. Milhano, M. Ploskon, and X. Zhang, Eur. Phys. J. C **78**, 529 (2018).
[22] M. Connors, C. Nattrass, R. Reed, and S. Salur, Rev. Mod. Phys. **90**, 025005 (2018).
[23] X. N. Wang, Z. Huang, and I. Sarcevic, Phys. Rev. Lett. **77**, 231 (1996).
[24] G. Y. Qin, J. Ruppert, C. Gale, S. Jeon, and G. D. Moore, Phys. Rev. C **80**, 054909 (2009).
[25] W. Dai, I. Vitev, and B. W. Zhang, Phys. Rev. Lett. **110**, 142001 (2013).
[26] X. N. Wang and Y. Zhu, Phys. Rev. Lett. **111**, 062301 (2013).
[27] L. Chen, G.-Y. Qin, L. Wang, S.-Y. Wei, B.-W. Xiao, H.-Z. Zhang, and Y.-Q. Zhang, Nucl. Phys. B **933**, 306 (2018).
[28] A. M. Sirunyan *et al.* (CMS Collaboration), Phys. Rev. Lett. **119**, 082301 (2017).
[29] R. B. Neufeld, I. Vitev, and B.-W. Zhang, Phys. Rev. C **83**, 034902 (2011).
[30] R. B. Neufeld and I. Vitev, Phys. Rev. Lett. **108**, 242001 (2012).
[31] Z. B. Kang, I. Vitev, and H. Xing, Phys. Rev. C **96**, 014912 (2017).
[32] J. Casalderrey-Solana, D. C. Gulhan, J. G. Milhano, D. Pablos, and K. Rajagopal, J. High Energy Phys. 03 (2016) 053.
[33] R. Kunnawalkam Elayavalli and K. C. Zapp, Eur. Phys. J. C **76**, 695 (2016).
[34] S. Chatrchyan *et al.* (CMS Collaboration), Phys. Lett. B **722**, 238 (2013).
[35] T. Gleisberg, S. Hoeche, F. Krauss, M. Schonherr, S. Schumann, F. Siegert, and J. Winter, J. High Energy Phys. 02 (2009) 007.
[36] Y. He, T. Luo, X. N. Wang, and Y. Zhu, Phys. Rev. C **91**, 054908 (2015).
[37] S. Cao, T. Luo, G. Y. Qin, and X. N. Wang, Phys. Rev. C **94**, 014909 (2016).
[38] L. Pang, Q. Wang, and X. N. Wang, Phys. Rev. C **86**, 024911 (2012).
[39] L. G. Pang, Y. Hatta, X. N. Wang, and B. W. Xiao, Phys. Rev. D **91**, 074027 (2015).
[40] S. Hoeche, F. Krauss, S. Schumann, and F. Siegert, J. High Energy Phys. 05 (2009) 053.
[41] S. Hoche, F. Krauss, M. Schonherr, and F. Siegert, J. High Energy Phys. 08 (2011) 123.
[42] S. Hoeche, F. Krauss, M. Schonherr, and F. Siegert, J. High Energy Phys. 04 (2013) 027.
[43] J. C. Collins, D. E. Soper, and G. F. Sterman, Nucl. Phys. B **250**, 199 (1985).
[44] T. Gleisberg and F. Krauss, Eur. Phys. J. C **53**, 501 (2008).
[45] S. Schumann and F. Krauss, J. High Energy Phys. 03 (2008) 038.
[46] J. C. Collins, J. High Energy Phys. 05 (2000) 004.
[47] Y. Chen, J. C. Collins, and N. Tkachuk, J. High Energy Phys. 06 (2001) 015.
[48] S. Hoeche, F. Krauss, M. Schonherr, and F. Siegert, J. High Energy Phys. 09 (2012) 049.
[49] F. Cascioli, P. Maierhofer, and S. Pozzorini, Phys. Rev. Lett. **108**, 111601 (2012).
[50] F. Krauss, R. Kuhn, and G. Soff, J. High Energy Phys. 02 (2002) 044.
[51] T. Gleisberg and S. Hoeche, J. High Energy Phys. 12 (2008) 039.
[52] M. Cacciari, G. P. Salam, and G. Soyez, Eur. Phys. J. C **72**, 1896 (2012).
[53] M. Cacciari, G. P. Salam, and G. Soyez, J. High Energy Phys. 04 (2008) 063.
[54] X. F. Guo and X. N. Wang, Phys. Rev. Lett. **85**, 3591 (2000).
[55] B. W. Zhang and X. N. Wang, Nucl. Phys. A **720**, 429 (2003).
[56] B. W. Zhang, E. Wang, and X. N. Wang, Phys. Rev. Lett. **93**, 072301 (2004).
[57] A. Majumder, Phys. Rev. D **85**, 014023 (2012).
[58] Z. W. Lin, C. M. Ko, B. A. Li, B. Zhang, and S. Pal, Phys. Rev. C **72**, 064901 (2005).
[59] W. Chen, S. Cao, T. Luo, L. G. Pang, and X. N. Wang, Phys. Lett. B **777**, 86 (2018).
[60] T. Luo, S. Cao, Y. He, and X. N. Wang, Phys. Lett. B **782**, 707 (2018).
[61] P. Ru, B. W. Zhang, L. Cheng, E. Wang, and W. N. Zhang, J. Phys. G **42**, 085104 (2015).
[62] O. Kodolova, I. Vardanyan, A. Nikitenko, and A. Oulianov, Eur. Phys. J. C **50**, 117 (2007).